Study of a magnetic-cooling material $Gd(OH)CO_3$†

Yan-Cong Chen,‡[a] Lei Qin,‡[b] Zhao-Sha Meng,[a] Ding-Feng Yang,[b] Chao Wu,*[b] Zhendong Fu,[c] Yan-Zhen Zheng,*[b] Jun-Liang Liu,[a] Róbert Tarasenko,[d] Martin Orendáč,*[d] Jan Prokleška,[e] Vladimír Sechovský[e] and Ming-Liang Tong*[a]

The magnetocaloric effect of a coordination polymeric material with a repeating unit of $Gd(OH)CO_3$ has been studied experimentally using isothermal magnetization and heat capacity measurements. The maximum entropy change, $-\Delta S_m$, reaches 66.4 J kg^{-1} K^{-1} or 355 mJ cm^{-3} K^{-1} for $\Delta H = 7$ T and $T = 1.8$ K. Density functional theory (DFT) calculations show weak and competing antiferromagnetic interactions between the metal centres.

Introduction

Since Warburg discovered the magnetocaloric effect (MCE) in metallic iron in 1881,[1] magnetic cooling has been proposed as an environmentally friendly and energy-efficient cooling technique.[2] Because the maximum MCE of a magnetic material usually occurs at the vicinity of the magnetic phase transition, the control of magnetic ordering is critical for certain applications.[3] At room temperature, the situation is challenging as there are not many ferromagnets which can order nearby.[4] For low temperatures more options are available because there is less thermal vibration from the lattice, thus, not only ferromagnets but also paramagnets can be employed. The discovery of gadolinium gallium garnet ($Gd_3Ga_5O_{12}$; GGG) and its iron-substituted derivative ($Gd_3(Ga_{1-x}Fe_x)_5O_{12}$:GGIG) have made it possible to have magnetic cooling applications from 2–20 K,[5] but there is still need for improvement (*i.e.*, to search for better replacements and/or extend the working region).[6]

Recently, a new type of nano-scale magnetic material has emerged in this field and has proved to be very competitive to GGG and GGIG as a low-temperature refrigerant.[7–10] Such new materials have distinct advantages, such as identical size, stoichiometric composition, and they provide the opportunity for rational synthesis and modification. The formulae for synthesizing such magnetic coolers have been reviewed recently,[11] from which it was noticed that much effort has been focused on enhancing the ground spin state (S) using the magnetic entropy change ($-\Delta S_m$) equation: $-\Delta S_m = R \ln(2S + 1)$, where R is the gas constant. The ion Gd^{3+} is, therefore, preferred for its half-filled 4f orbital ($S = 7/2$) and magnetic isotropy. But Gd^{3+} has the disadvantage of a large atomic weight because the gravimetric $-\Delta S_m$ is inversely proportional to the molecular weight. Moreover, as the internal 4f electrons are well covered by outer paired electrons the magnetic communications between the Gd^{3+} ions are usually weak. As such, MCE contributed from phase transition is usually minor, and better Gd(III)-based magnetic coolers (there is no difference whether this is determined gravimetrically or volumetrically) are always commensurate with a high metal/ligand ratio.

This could be realized by using low molecular mass ligands or increasing the dimensionality or building Gd(III)-based coordination polymers.[9,10] To achieve this goal, a ligand with a multi-negative charge and a high coordination number is important for counterbalancing the positive charges and meeting the high coordination requirement of the Gd^{3+} ions. To date, carboxylate ligands, especially small acetates and formates are preferred for this purpose,[10] and the large metal/ligand ratio further leads to a high mass density which is responsible for a greater volumetric MCE.[12] Instead of using these carboxylate ligands, in this paper it is proposed that carbonate ligands are used instead, because carbonate can be regarded as a condensation product of carboxylates by reducing the non-coordinating moiety, see Scheme 1. It was expected that the high negative charge and multi-coordination sites would make CO_3^{2-} more efficient than formate and oxalate when binding Gd^{3+} ions. Moreover,

[a]*Key Laboratory of Bioinorganic and Synthetic Chemistry of Ministry of Education, State Key Laboratory of Optoelectronic Materials and Technologies, School of Chemistry & Chemical Engineering, Sun Yat-Sen University, Guangzhou, 510275, China. E-mail: tongml@mail.sysu.edu.cn*

[b]*Frontier Institute of Science and Technology, and College and Science, Xi'an Jiaotong University, Xi'an 710054, China. E-mail: chaowu@mail.xjtu.edu.cn; zheng.yanzhen@mail.xjtu.edu.cn*

[c]*Institut für Festkörperforschung, Forschungszentrum Jülich, 52425 Jülich, Germany*

[d]*Centre of Low Temperature Physics Faculty of Science, P.J. Šafárik University and Institute of Experimental Physics SAS, Park Angelinum 9, 041 54 Košice, Slovakia. E-mail: martin.orendac@upjs.sk*

[e]*Faculty of Mathematics and Physics, Department of Condensed Matter Physics, Charles University, Ke Karlovu 5, CZ-12116 Prague 2, Czech Republic*

† Electronic supplementary information (ESI) available: Additional crystallography tables and figures of magnetic properties.

‡ These two authors contributed equally.

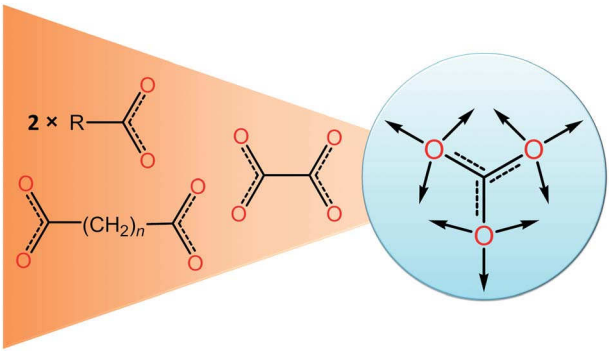

Scheme 1 A comparison of carboxylate and carbonate. Arrows are the available coordination sites.

the coordination topology of CO_3^{2-} based on its triangular shape shows promise for inducing competing magnetic interactions between the metal centres, such as geometrical spin frustration, which is believed to be beneficial for enhancing MCE.[11]

Driven by these two reasons, a Gd(III) hydroxyl carbonate with a repeating unit of $Gd(OH)CO_3$ was synthesized. This material exhibits maximum magnetic entropy change, $-\Delta S_m$, up to 67.1 J kg^{-1} K^{-1} (or 359 mJ cm^{-3} K^{-1}) and the adiabatic temperature change (ΔT_{ad}) was up to 24 K for $\Delta H = 9$ T, which is comparable to the performance of GGG or GGIG.

Experimental section

Synthesis of $Gd(OH)CO_3$

Method A. A mixture of $GdCl_3 \cdot 6H_2O$ (0.1 mmol), malononitrile (0.2 mmol) and deionized water (5 mL) was sealed into a 23 mL Teflon-lined autoclave and heated at 180 °C for 72 h, followed by cooling to room temperature in air. Colourless crystals were washed with deionized water and dried in air (yield 50% based on Gd).

Method B. $GdCl_3 \cdot 6H_2O$ (2.0 mmol) and Na_2CO_3 (2.0 mmol) were mixed in H_2O (40 mL) and stirred for 15 minutes at room temperature. The slurry was sealed into a 50 mL Teflon-lined autoclave and heated at 170 °C for 72 h, followed by cooling to room temperature at a rate of 3 °C h^{-1}. Colourless, block shaped crystals were isolated and washed with deionized water (yield 52.8% based on Gd).

IR data of $Gd(OH)CO_3$ (KBr cm^{-1}): 3459 (s), 2521 (w), 2340 (w), 1825 (s), 1790 (s). The calculated analysis for $CHGdO_4$ was: C 5.13, H 0.43; the experimental analysis was: C 5.31, H 0.56.

X-ray crystallography

Powder X-ray diffraction measurements were performed on ground polycrystalline samples at room temperature on a D8 X-Ray Diffractometer (Bruker) with Cu Kα radiation. Single-crystal diffraction data was recorded at 150(2) K on an R-AXIS SPIDER Image Plate diffractometer (Rigaku) with Mo Kα radiation, solved by direct methods and refined using SHELXTL program (Georg-August-Universität Göttingen).[13a] The metrical symmetry and space group data were confirmed using the PLATON program (University of Glasgow).[13b] Crystal data and structural refinement data are listed in Table 1. Further details on the crystal structure may be obtained in the ESI (Tables S1 and S2†) and from the Fachinformationszentrum Karlsruhe, 76344 Eggenstein-Leopoldshafen, Germany (fax: (+49)7247-808-666; e-mail: crysdata@fiz-karlsruhe.de), by quoting the depository number CSD-426257 ($Gd(OH)CO_3$).

Table 1 Crystal data and structural refinement

Chemical formula	$CHGdO_4$
Formula mass/g mol^{-1}	234.27
Crystal system	Orthorhombic
Space group	*Pnma*
Z	4
a/Å	7.0770(7)
b/Å	4.8730(9)
c/Å	8.4353(6)
Unit cell volume/$Å^3$	290.90(6)
Temperature/K	150(2)
ρ_{calcd}/g cm^{-3}	5.349
μ (Mo Kα)/mm^{-1}	22.608
No. of reflections measured	2591
No. of independent reflections	356
R_{int}	0.0305
R_1[a] ($I > 2\sigma(I)$)	0.0201
wR_2[b] (all data)	0.0538
Goodness of fit on F^2	1.036

[a] $R_1 = \sum||F_o| - |F_c||/\sum|F_o|$. [b] $wR_2 = [\sum w(F_o^2 - F_c^2)^2/\sum w(F_o^2)^2]^{1/2}$.

Physical measurements

The magnetic measurements of the polycrystalline samples were performed using a MPMS XL-7 SQUID (Quantum Design) magnetometer. Low temperature magnetic susceptibility was measured on the polycrystalline samples synthesized using method B. Low temperature specific heat was studied on a Quantum Design PPMS® using the ^{3}He option with the standard relaxation technique.

Density functional theory (DFT) calculations

DFT calculations were performed with CASTEP code.[14a] The crystal structure of $Gd(OH)CO_3$ determined from single-crystal X-ray diffraction was employed for theoretical studies without further geometrical optimization. Ultra-soft pseudopotentials were utilized to describe the electron ion interactions. Exchange and correlation were described by a Perdew–Burke–Ernzerhof function in the generalized gradient approximation (GGA) scheme.[14b] A kinetic energy cut-off of 600 eV was used for plane-wave expansions in the reciprocal space. The Monkhorst–Pack grid was set to 5 × 5 × 5 in the Brillouin zone of the 1 × 2 × 1 supercell.[14c] Our spin-polarized calculations predicted that $Gd(OH)CO_3$ is a magnetic insulator even without adding on site repulsion, U, on Gd, which can be seen from the total and partial DOS plots calculated for the ferromagnetic state of $Gd(OH)CO_3$ in Fig. S4,† so we did not use the DFT plus U method.[14d]

Results and discussion

Synthesis

There are two hydrothermal methods for the synthesis of $Gd(OH)CO_3$. Method A involves the decomposition of malononitrile ($NC–CH_2–CN$). It is easy for cyano groups to be hydrolysed into carboxylates and amines in the hydrothermal condition ($R–CN \rightarrow R–CONH_2 \rightarrow R–COO^- + NH_4^+$). The former product can be further decomposed to CO_3^{2-} *via* decarboxylation and thus, the $Gd(OH)CO_3$ precipitates out. The amine can act as a buffering agent to prevent the rapid hydrolysis of Gd^{3+} into $Gd(OH)_3$ or other products. Method B which involves the direct reaction of Gd^{3+} ions and carbonates is also very efficient.

Crystal structure

The powder X-ray diffraction pattern of $Gd(OH)CO_3$ has been known for decades as it has been listed in JCPDF (#43-0604, unindexed) with a provisional formula of $Gd_2O(CO_3)_2 \cdot H_2O$. However, such an assignment cannot explain the high thermal stability of this material, which is up to ~700 K.[15a] Without single-crystal X-ray data, the exact structure remains controversial and the crystallization into orthorhombic $P2_12_12_1$ (ref. 15b) and hexagonal $P\bar{6}$ (ref. 15c) space groups have also been reported. Our single-crystal diffraction data analysis reveals that $Gd(OH)CO_3$ crystallizes in the orthorhombic space group *Pnma via* the hydrothermal synthesis described previously, without producing the other phases, as shown in Fig. 1.

In the crystal structure, each asymmetric unit contains half of the chemical formula. The Gd^{3+} ion is 10-coordinated with six oxygen atoms from three chelating CO_3^{2-} groups, two oxygen atoms from two mono-dentate CO_3^{2-} groups, and the other two oxygen atoms are from two OH^- groups. The Gd···O separations range from 2.29 to 2.75 Å (Fig. 2a). The CO_3^{2-} groups are μ_5-bridging with two μ_3-O and one μ-O atoms bound to adjacent Gd^{3+} ions (Fig. 2b), and the hydroxyl groups are μ-bridging between Gd^{3+}, forming one-dimensional (1D) zigzag [–Gd–(μ-OH)–Gd–(μ-OH)]$_n$ chains along the *a* axis with a Gd···Gd separation of 3.82 Å (Fig. 3).

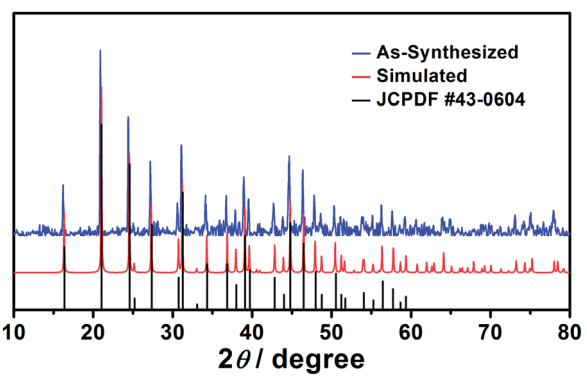

Fig. 1 Powder XRD pattern of as-synthesized $Gd(OH)CO_3$ compared to the simulation from the single crystal structure and JCPDF #43-0604.

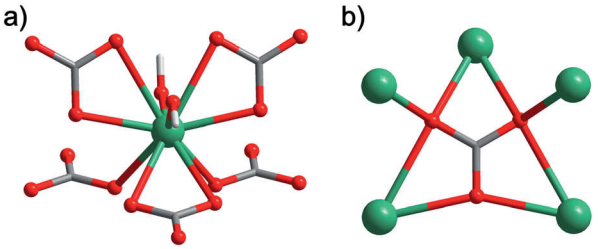

Fig. 2 The coordination environment of (a) Gd^{3+} and (b) CO_3^{2-}. Colour codes: Gd, green; O, red; C, grey; H, light grey.

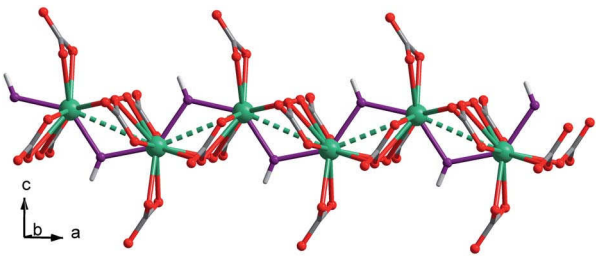

Fig. 3 The 1D Gd^{3+}–OH^- zigzag chain along the *a* axis. Colour codes: Gd, green; O, red and purple; C, grey; H, light light grey.

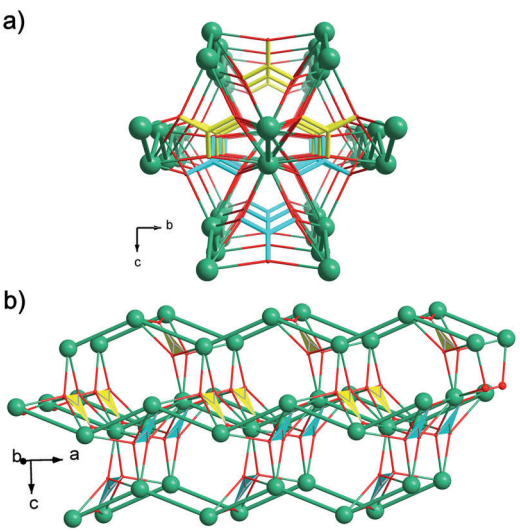

Fig. 4 The inter-chain structure supported by CO_3^{2-} viewed (a) along the *a* axis and (b) aside from the *b* axis. The OH^- groups are omitted for clarity and the opposite carbonates are highlighted with yellow and blue triangles. Colour codes: Gd, green; O, red; C, yellow, light blue and grey.

The network structure of $Gd(OH)CO_3$ can be depicted in two ways depending on the building units used. One way is to use the [–Gd–(μ-OH)–Gd–(μ-OH)]$_n$ chains as building units. Each of them is interlinked with six neighbours into a three-dimensional (3D) network (Fig. 4a). However, the six linking directions are inequivalent. Four of them are only directed by a pair of μ_3-O atoms from the μ_5-CO_3^{2-} groups in adjacent *ab*-plane. The other two directions are extended in the *ab*-plane. As shown in Fig. 4b,

the zigzag [–Gd–(μ-OH)–Gd–(μ-OH)]$_n$ chains are alternatively linked by opposite carbonate groups. Thus, the other way to describe the 3D structure is to use the *ab* planes as building units, which contain exactly the formula [Gd(OH)CO$_3$]$_n$.

The dense inorganic structure of the Gd(OH)CO$_3$ framework without solvent-accessible porosity gives rise to a large density of 5.349 g cm^{-3}, which is beneficial for the volumetric MCE. Furthermore, it was found that the hydroxyl groups in the structure are μ-bridging rather than μ$_3$-bridging, and such a bridging mode may weaken the magnetic coupling between the Gd^{3+} ions, thus this structure is extremely favourable for a cryogenic magnetic cooler.

Magnetic properties

Variable temperature magnetic susceptibility measurements were performed on a polycrystalline sample of Gd(OH)CO$_3$ in an applied dc field of 0.05 T (Fig. 5a). At room temperature, the $\chi_m T$ value is 7.84 cm^3 K mol^{-1}, which is in good agreement with the spin-only value expected for a free Gd^{3+} ion with $g = 2$ (7.875 cm^3 K mol^{-1}). Upon cooling, the $\chi_m T$ essentially stays constant until approximately 30 K, which is then followed by a gradual decrease to the minimum of 4.68 cm^3 K mol^{-1} at 1.8 K. The inverse magnetic susceptibility ($1/\chi_m$) obeys the Curie–Weiss law with $C = 7.86$ cm^3 K mol^{-1} and $\theta = -1.05$ K, indicating a weak antiferromagnetic coupling. Surprisingly, despite the large proportion of OH^- in the polymeric structure, the overall magnetic coupling characterized by the Weiss constant θ is weaker than in many molecular clusters and cluster-organic frameworks comprising Gd^{3+}. Such a behaviour not only arises from the difference between the μ-OH^- and the μ$_3$-OH^- bridges, but is also due to the competing magnetic interactions mediated by the CO_3^{2-} groups.

The isothermal magnetization from 1.8 K to 8.2 K were also measured (Fig. 5b). The magnetization increases steadily with the applied dc field and reaches the saturation value of 7.0 Nβ at 1.8 K and 7 T, which is in good agreement with the expected value for a Gd^{3+} ion ($s = 7/2$, $g = 2$). The large magnetization values, together with the low molecular weight and high mass density, make this material a promising candidate for cryogenic magnetic refrigeration, where the isothermal entropy change can be calculated by applying the Maxwell equation (Fig. 6):

$$\Delta S_m(T) = \int_0^H [\partial M(T,H)/\partial T]_H \mathrm{d}H$$

In general, the $-\Delta S_m$ values increase gradually as the temperature is reduced, but rise progressively with increasing applied fields, reaching a maximum of 66.4 J kg^{-1} K^{-1} (355 mJ cm^{-3} K^{-1}) at $T = 1.8$ K and $\Delta H = 7$ T, which is close to the theoretical limiting value of 73.8 J kg^{-1} K^{-1} (395 mJ cm^{-3} K^{-1}) calculated from $R \ln(2s + 1)/M_w$ with $s = 7/2$ and $M_w = 234.3$ g mol^{-1}. This result is quite exciting, however, the peak of $-\Delta S_m$ is still not reached at the aforementioned temperature, indicating the necessity of further investigation in the sub-Kelvin region.

Heat capacity

To further investigate the MCE of this material, low temperature heat capacity (C) measurements were performed in the applied fields from 0 to 9 T (Fig. 7). Clearly, the higher temperature region is dominated by a lattice contribution arising from the thermal vibration, which fits well to the Debye's model and yield the Debye temperature (θ_D) of 313(3) K with $r_D = 7$.[16] Such a high Debye temperature compared to that obtained with other

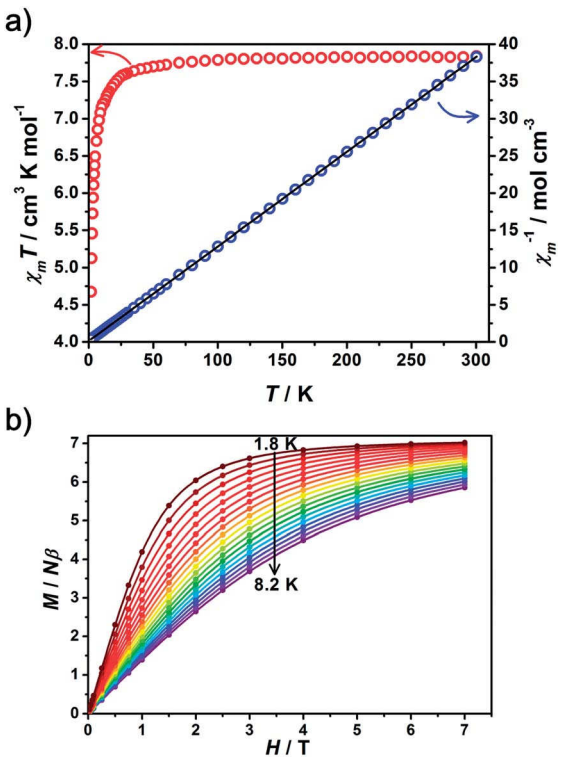

Fig. 5 (a) Temperature-dependencies of the magnetic susceptibility product, $\chi_m T$, and the inverse magnetic susceptibility, $1/\chi_m$, at 1.8–300 K with a dc field of 0.05 T. The black solid line represents the least-square fit for the Curie–Weiss law. (b) Magnetization *versus* the dc field in the temperature range of 1.8–8.2 K.

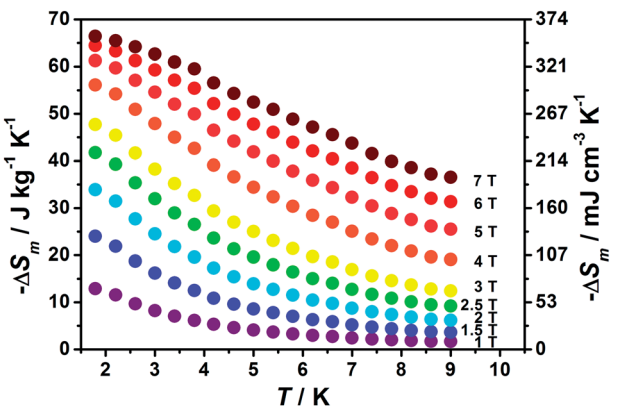

Fig. 6 Temperature-dependencies of $-\Delta S_m$ for selected ΔH obtained from magnetization. The data with field variation below 1 T are omitted for clarity.

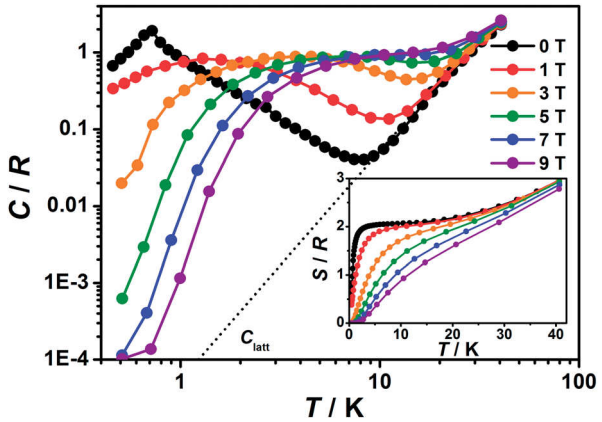

Fig. 7 Temperature-dependencies of the heat capacity normalized to the gas constant at selected applied fields. The dotted line represent the lattice contribution. Inset: temperature-dependencies of the entropy obtained from the heat capacity.

molecule-based materials is indicative of the rigid frameworks consisting of strong chemical bonds and light ligand atoms.[10] This is very important to yield a large ΔT_{ad} in the adiabatic demagnetization process, where the lattice vibration is forced to compensate for the variation of magnetic entropy.

At lower temperatures, the heat capacity is dominated by the field-dependent magnetic contribution, which shows a broad Schottky type feature caused by the splitting of the $^8S_{7/2}$ multiplet. A small sharp anomaly is observed in the zero field at approximately 0.7 K but is suppressed by the applied fields, indicating the emergence of a phase transition. This can be attributed to the long range magnetic interactions mediated by the polymeric network, which is further demonstrated to be antiferromagnetic by a downturn on the $\chi_m T$ curve (Fig. S1†). Such a behaviour is also observed in the recently reported $Gd(HCOO)_3$ of around 0.8 K,[10d] however, the entropy content associated with the magnetic transition is quite low and it makes little impact on the cooling capability as we can see below.

From the experimental C, the entropy can be obtained by a numerical integration using:

$$S(T) = \int_0^T C(T)/T \mathrm{d}T$$

The experimental value of C were subsequently extrapolated, and a constant value base on the high temperature saturation value of magnetic entropy ($S_{m,sat} = R\ln(2s + 1) = 2.08\ R$), Fig. S2† was added to the zero-field entropy to compensate for the experimental inaccessibility to absolute zero.[10a] Thus, the isothermal magnetic entropy change (ΔS_m) and the adiabatic temperature change (ΔT_{ad}) can be derived from the S–T curves (inset of Fig. 7) by vertical and horizontal subtraction, respectively.[4]

The maxima of the temperature-dependencies of $-\Delta S_m$ keep rising and shift to higher temperatures with increasing applied fields (Fig. 8). Indeed, the $-\Delta S_{m,max}$ for $\Delta H = 1$ T is already up to 26.2 J kg^{-1} K^{-1} (140 mJ cm^{-3} K^{-1}), and it increases sharply

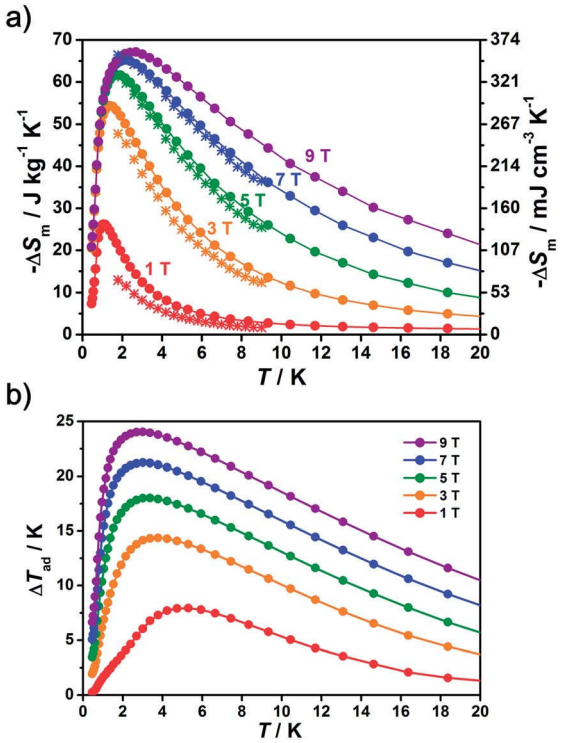

Fig. 8 (a) Temperature-dependencies of $-\Delta S_m$ obtained from magnetization (★) and heat capacity (●) for selected ΔH. (b) Temperature-dependencies of ΔT_{ad} for selected ΔH.

when higher fields are applied, namely 54.4 J kg^{-1} K^{-1} (291 mJ cm^{-3} K^{-1}) for $\Delta H = 3$ T and 67.1 J kg^{-1} K^{-1} (359 mJ cm^{-3} K^{-1}) for $\Delta H = 9$ T (Table 2).

Because of the advantages of high spin density (Gd^{3+} takes up 67% (mass fraction) in the formula $CHGdO_4$) and mass density (5.349 g cm^{-3}), the performance of $Gd(OH)CO_3$ is excellent in both the gravimetric and volumetric results (Fig. 9). Indeed, it not only surpasses the former reported records with a $-\Delta S_{m,max}$ of 60.3 J kg^{-1} K^{-1} ($[Mn(glc)_2(H_2O)_2]$)[7g] and 144 mJ cm^{-3} K^{-1} ($[Gd_6(OH)_8(suc)_5(H_2O)_2]_n \cdot 4nH_2O$),[9h] but also exceeds

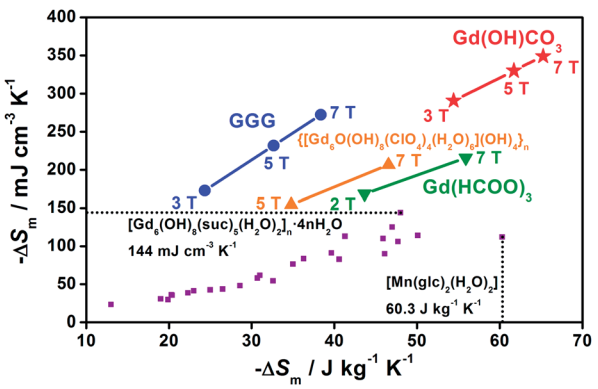

Fig. 9 Comparison of the maximum $-\Delta S_m$ with selected ΔH for $Gd(OH)CO_3$(★), $Gd(HCOO)_3$ (▼),[10d] $\{[Gd_6O(OH)_8(ClO_4)_4(H_2O)_6](OH)_4\}_n$ (▲),[9g] GGG (●) and the recently reported molecule-based magnetic refrigerants (■, $\Delta H = 7$ T).

Table 2 Magnetic entropy change for selected molecule-based materials[a]

Complex[ref.]	ΔH (T)	$-\Delta S_{m,max}$ (J kg^{-1} K^{-1})	$-\Delta S_{m,max}$ (mJ cm^{-3} K^{-1})
3d type			
$\{Mn^{III}_6Mn^{II}_4\}$[7a,b]	7	13.0	20.9
$\{Mn^{III}_{11}Mn^{II}_6\}$[7c]	7	13.3	21.8
$\{Mn^{III}_6Mn^{II}_4\}$[7b]	7	17.0	26.2
$\{Mn^{II}_4\}$[7d]	5	19.3	33.3
$\{Fe^{III}_{14}\}$[7e]	7	20.3	42.2
$\{Mn^{III}_6Mn^{II}_8\}$[7b]	7	25.0	42.5
$[Mn^{II}(Me\text{-}ip)(DMF)]_n$[7f]	8	42.4	66.7
$[Mn^{II}(glc)_2(H_2O)_2]$[7g]	7	60.3	112
3d–4f type			
$\{Co^{II}_4Gd^{III}_{10}\}$[8k]	7	32.6	54.3
$\{Cu^{II}_5Gd^{III}_4\}$[8c]	9	31.0	61.7
$\{Ni^{II}_{12}Gd^{III}_{36}\}$[8e]	7	36.3	83.5
$\{Co^{II}_{10}Gd^{III}_{42}\}$[8h]	7	41.3	113
$\{[Mn^{II}(H_2O)_6][Mn^{II}Gd^{III}(oda)_3]_2\cdot 6H_2O\}_n$[8j]	7	50.1	114
4f type			
$\{[Gd^{III}_{36}(NA)_{36}(OH)_{49}(O)_6(NO_3)_6(N_3)_3(H_2O)_{20}]Cl_2\cdot 28H_2O\}_n$[9c]	7	39.7	91.3
$\{[Gd^{III}_2(IDA)_3]\cdot 2H_2O\}_n$[9d]	7	40.6	101
$[Gd^{III}(OAc)_3(H_2O)_{0.5}]_n$[10b]	7	47.7	106
$[Gd^{III}(HCOO)(OAc)_2(H_2O)_2]_n$[10c]	7	45.9	110
$[Gd^{III}(C_4O_4)(OH)(H_2O)_4]_n$[9e]	9	47.3	113
$\{Gd^{III}_{48}\}$[9i]	7	43.6	121
$[Gd^{III}(HCOO)(bdc)]_n$[9b]	9	47.0	125
$[Gd^{III}_6(OH)_8(suc)_5(H_2O)_2]_n$[9h]	7	48.0	144
$\{[Gd^{III}_6O(OH)_8(ClO_4)_4(H_2O)_6](OH)_4\}_n$[9g]	7	46.6	207
$[Gd^{III}(HCOO)_3]_n$[10d]	7	55.9	216
$[Gd^{III}(OH)CO_3]_n$ (this work)	3	54.4	291
	5	61.7	330
	7	66.4	355

[a] Me-ip = 5-methylisophthalate, DMF = dimethylformamide, glc = glycolate, oda = oxydiacetate, NA = nicotinate, IDA = iminodiacetate, bdc = benzenedicarboxylate, suc = succinate.

the recently reported values of $\{[Gd_6O(OH)_8(ClO_4)_4(H_2O)_6](OH)_4\}_n$ ($-\Delta S_{m,max} = 207$ mJ cm^{-3} K^{-1})[9g] and $Gd(HCOO)_3$ ($-\Delta S_{m,max} = 215.7$ mJ cm^{-3} K^{-1}).[10d]

Because the use of a high magnetic field may not be suitable in all circumstances from the technical and economic viewpoint, the cooling capability under modest fields is of great importance. In this research $Gd(OH)CO_3$ is also found to be excellent, *e.g.*, it already surpasses commercial GGG whose $-\Delta S_{m,max} \approx 24$ J kg^{-1} K^{-1} (173 mJ cm^{-3} K^{-1}) for $\Delta H = 3$ T.[5] This prominent feature, along with the remarkable ΔS_m and ΔT_{ad} obtained in a higher applied field, further highlights the promising cooling power and energy efficiency of $Gd(OH)CO_3$.

DFT calculation

To provide clarification of the magnetic interactions between the Gd(III) ions, a theoretical calculation using the DFT-GGA

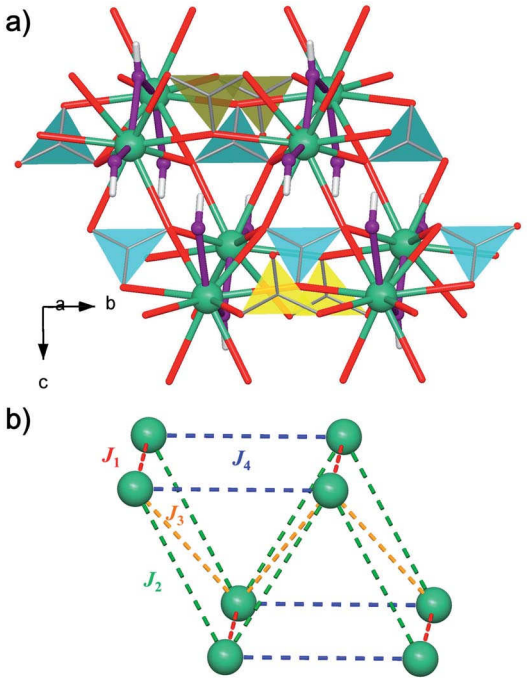

Fig. 10 (a) A (*a* 2*b* *c*) supercell of $Gd(OH)CO_3$ showing the exchange pathways by OH^- (purple chains) and CO_3^{2-} (blue and yellow triangles). Colour codes: Gd, green; O, red and purple; C, grey; H, light grey. (b) Magnetic coupling interactions J_1–J_4 between Gd^{3+} ions.

method with CASTEP code was performed.[14] Four different Gd–O–Gd coupling interactions, J_1–J_4, between Gd^{3+} ions in a (*a* 2*b* *c*) supercell (Fig. 10 and S3a†) are considered. J_1 is the intra-chain exchange mediated by both OH^- and CO_3^{2-} groups, while J_2–J_4 are the inter-chain exchange through CO_3^{2-} only. To determine the values of these exchange parameters, five ordered spin states were built (Fig. S3b–f†) and the energy differences were calculated according to the following Hamiltonian:

$$\hat{H} = -\sum_{i<j} J_{ij} S_i S_j$$

where J_{ij} (= J_1, J_2, J_3, J_4) is the magnetic exchange-coupling constants between the spin sites i and j, and S_i and S_j are the spin angular momentum operators at the spin sites i and j, respectively.

By applying the energy expressions obtained for spin dimers with N unpaired spins per spin site (in the present case, $N = 7$), the total spin exchange energies per unit cell of the five spin states are written as:

$$E_{FM} = (-4J_1 - 6J_2 - 3J_3 - 4J_4) \times N^2/4$$

$$E_{AFM1} = (-4J_1 + 6J_2 + 3J_3 - 4J_4) \times N^2/4$$

$$E_{AFM2} = (4J_1 - 6J_2 + 3J_3 - 4J_4) \times N^2/4$$

$$E_{AFM3} = (4J_1 + 6J_2 - 3J_3 - 4J_4) \times N^2/4$$

$$E_{AFM4} = (-4J_1 - 2J_2 - J_3 + 4J_4) \times N^2/4$$

Table 3 Geometrical parameters associated with spin exchange paths, J_1–J_4, in a double unit cell (*a* 2*b* *c*) of $Gd(OH)CO_3$ and values of J_1–J_4 calculated from the DFT-GGA method

	Distance (Å)	Type of Gd–O–Gd bridges			J (cm^{-1})
Exchange	Gd–O–Gd	μ-OH^-	μ-O (CO_3^{2-})	μ_3-O (CO_3^{2-})	$U = 0$
J_1	3.825	1	0	2	−0.163
J_2	5.128	0	0	1	−0.041
J_3	4.207	0	0	2	0.076
J_4	4.885	0	1	0	−0.073

By mapping the relative energies of the five ordered spin states determined from the GGA calculations, the values (in cm^{-1}) of J_1, J_2, J_3, and J_4 obtained were −0.163, −0.041, 0.076 and −0.073, respectively (Table 3). To check whether these values were reasonable, the Weiss constant θ calculated from the J values obtained and the experimental fit were compared. According to the mean field theory[14] θ and J are related by:

$$\theta = \frac{s(s+1)}{3k_B} \sum_i z_i J_i$$

where the summation runs over all the nearest neighbours of a given spin site, and z_i is the number of nearest neighbours connected by the spin exchange parameter J_i. Thus, θ can be approximated as:

$$\theta \approx \frac{63(2J_1 + 2J_2 + 2J_3 + 2J_4)}{12k_B}$$

The θ value obtained was −3.0 K, which fits well with the experimental result of −1.05 K because the GGA calculations usually overestimate the spin exchange interaction.[17a] From the above calculations, it can be seen that all the spin interactions are very weak because of the internal nature of 4f electrons, which were also observed in other gadolinium compounds.[17b,c] The negative value of J_1 accounts for the strongest antiferromagnetic interaction along the Gd^{3+}–OH^- chains, which dominate the magnetic states of $Gd(OH)CO_3$. However, the positive J_3 shows non-negligible inter chain ferromagnetism. Moreover, the antiferromagnetic J_2 and J_4 lead to competing exchange-coupling interactions in the triangular J_2–J_2–J_4 substructure, and thus on the *bc* plane.[17d] Usually, spin-competition may lead to a large number of degenerate spin-states and delay the magnetic ordering, which is beneficial to enhancing the MCE.

Conclusions

In this study, the single-crystal structure and the experimental evaluation of the magnetocaloric effect of a polymeric coordination material, the orthorhombic $Gd(OH)CO_3$, was demonstrated by magnetization and heat capacity measurements. It was found that it makes no difference whether low or high fields are used, the MCE of $Gd(OH)CO_3$ compares well to the commercially available material, GGG, which makes it a promising material for cryogenic magnetic cooling applications.

Acknowledgements

This work was supported by the "973 Project" (2012CB821704 and 2014CB845602), project NSFC (Grant no. 91122032, 21371183, 21121061 and 21201137), the NSF of Guangdong (S2013020013002), Program for Changjiang Scholars and Innovative Research Team in University of China (IRT1298), project APVV-0132-11 and the "National 1000 Young Talents" program. Part of the thermodynamic studies was performed in MLTL (http://mltl.eu/), which is supported within the program of Czech Research Infrastructures (project no. LM2011025).

Notes and references

1 E. Warburg, *Ann. Phys.*, 1881, **249**, 141.
2 P. Debye, *Ann. Phys.*, 1926, **386**, 1154.
3 W. F. Giauque, *J. Am. Chem. Soc.*, 1927, **49**, 1864.
4 V. K. Pecharsky and K. A. Gschneidner Jr, *J. Magn. Magn. Mater.*, 1999, **200**, 44.
5 B. Baudun, R. Lagnier and B. Salce, *J. Magn. Magn. Mater.*, 1982, **27**, 315.
6 V. Franco, J. S. Blázquez, B. Ingale and A. Conde, *Annu. Rev. Mater. Res.*, 2012, **42**, 305.
7 (*a*) M. Manoli, R. D. L. Johnstone, S. Parsons, M. Murrie, M. Affronte, M. Evangelisti and E. K. Brechin, *Angew. Chem., Int. Ed.*, 2007, **119**, 4540; (*b*) M. Manoli, A. Collins, S. Parsons, A. Candini, M. Evangelisti and E. K. Brechin, *J. Am. Chem. Soc.*, 2008, **130**, 11129; (*c*) S. Nayak, M. Evangelisti, A. K. Powell and J. Reedijk, *Chem.–Eur. J.*, 2010, **16**, 12865; (*d*) J.-P. Zhao, R. Zhao, Q. Yang, B.-W. Hu, F.-C. Liu and X.-H. Bu, *Dalton Trans.*, 2013, **42**, 14509; (*e*) R. Shaw, R. H. Laye, L. F. Jones, D. M. Low, C. Talbot-Eeckelaers, Q. Wei, C. J. Milios, S. Teat, M. Helliwell, J. Raftery, M. Evangelisti, M. Affronte, D. Collison, E. K. Brechin and E. J. L. McInnes, *Inorg. Chem.*, 2007, **46**, 4968; (*f*) C.-B. Tian, R.-P. Chen, C. He, W.-J. Li, Q. Wei, X.-D. Zhang and S.-W. Du, *Chem. Commun.*, 2014, **50**, 1915; (*g*) Y.-C. Chen, J.-L. Liu, J.-D. Leng, F.-S. Guo, P. Vrábel, M. Orendáč, J. Prokleška, V. Sechovský and M.-L. Tong, *Chem.–Eur. J.*, 2014, **20**, 3029.
8 (*a*) G. Karotsis, M. Evangelisti, S. J. Dalgarno and E. K. Brechin, *Angew. Chem., Int. Ed.*, 2009, **48**, 9928; (*b*) G. Karotsis, S. Kennedy, S. J. Teat, C. M. Beavers, D. A. Fowler, J. J. Morales, M. Evangelisti, S. J. Dalgarno and E. K. Brechin, *J. Am. Chem. Soc.*, 2010, **132**, 12983; (*c*) S. K. Langley, N. F. Chilton, B. Moubaraki, T. Hooper, E. K. Brechin, M. Evangelisti and K. S. Murray, *Chem. Sci.*, 2011, **2**, 1166; (*d*) Y.-Z. Zheng, M. Evangelisti and R. E. P. Winpenny, *Angew. Chem., Int. Ed.*, 2011, **50**, 3692; (*e*) J.-B. Peng, Q.-C. Zhang, X.-J. Kong, Y.-P. Ren, L.-S. Long, R.-B. Huang, L.-S. Zheng and Z. Zheng, *Angew. Chem., Int. Ed.*, 2011, **50**, 10649; (*f*) T. N. Hooper,

J. Schnack, S. Piligkos, M. Evangelisti and E. K. Brechin, *Angew. Chem., Int. Ed.*, 2012, **51**, 4633; (*g*) Y.-Z. Zheng, M. Evangelisti, F. Tuna and R. E. P. Winpenny, *J. Am. Chem. Soc.*, 2012, **134**, 1057; (*h*) J.-B. Peng, Q.-C. Zhang, X.-J. Kong, Y.-Z. Zheng, Y.-P. Ren, L.-S. Long, R.-B. Huang, L.-S. Zheng and Z. Zheng, *J. Am. Chem. Soc.*, 2012, **134**, 3314; (*i*) J.-D. Leng, J.-L. Liu and M.-L. Tong, *Chem. Commun.*, 2012, **48**, 5286; (*j*) F.-S. Guo, Y.-C. Chen, J.-L. Liu, J.-D. Leng, Z.-S. Meng, P. Vrábel, M. Orendáč and M.-L. Tong, *Chem. Commun.*, 2012, **48**, 12219; (*k*) E. M. Pineda, F. Tuna, R. G. Pritchard, A. C. Regan, R. E. P. Winpenny and E. J. L. McInnes, *Chem. Commun.*, 2013, **49**, 3522; (*l*) J.-L. Liu, Y.-C. Chen, Q.-W. Li, S. Gómez-Coca, D. Aravena, E. Ruiz, W.-Q. Lin, J.-D. Leng and M.-L. Tong, *Chem. Commun.*, 2013, **49**, 6549; (*m*) Z.-M. Zhang, L.-Y. Pan, W.-Q. Lin, J.-D. Leng, F.-S. Guo, Y.-C. Chen, J.-L. Liu and M.-L. Tong, *Chem. Commun.*, 2013, **49**, 8081; (*n*) J.-L. Liu, Y.-C. Chen, Q.-W. Li, S. Gómez-Coca, D. Aravena, E. Ruiz, J.-D. Leng and M.-L. Tong, *Chem.–Eur. J.*, 2013, **19**, 17567.

9 (*a*) R. J. Blagg, F. Tuna, E. J. L. McInnes and R. E. P. Winpenny, *Chem. Commun.*, 2011, **47**, 10587; (*b*) R. Sibille, T. Mazet, B. Malaman and M. François, *Chem.–Eur. J.*, 2012, **18**, 12970; (*c*) M. Wu, F. Jiang, X. Kong, D. Yuan, L. Long, S. A. Al-Thabaiti and M. Hong, *Chem. Sci.*, 2013, **4**, 3104; (*d*) J.-M. Jia, S.-J. Liu, Y. Cui, S.-D. Han, T.-L. Hu and X.-H. Bu, *Cryst. Growth Des.*, 2013, **13**, 4631; (*e*) S. Biswas, A. Adhikary, S. Goswami and S. Konar, *Dalton Trans.*, 2013, **42**, 13331; (*f*) L.-X. Chang, G. Xiong, L. Wang, P. Cheng and B. Zhao, *Chem. Commun.*, 2013, **49**, 1055; (*g*) Y.-L. Hou, G. Xiong, P.-F. Shi, R.-R. Cheng, J.-Z. Cui and B. Zhao, *Chem. Commun.*, 2013, **49**, 6066; (*h*) Y.-C. Chen, F.-S. Guo, Y.-Z. Zheng, J.-L. Liu, J.-D. Leng, R. Tarasenko, M. Orendáč, J. Prokleška, V. Sechovský and M.-L. Tong, *Chem.–Eur. J.*, 2013, **19**, 13504; (*i*) F.-S. Guo, Y.-C. Chen, L.-L. Mao, W.-Q. Lin, J.-D. Leng, R. Tarasenko, M. Orendáč, J. Prokleška, V. Sechovský and M.-L. Tong, *Chem.–Eur. J.*, 2013, **19**, 14876.

10 (*a*) M. Evangelisti, O. Roubeau, E. Palacios, A. Camín, T. N. Hooper, E. K. Brechin and J. J. Alonso, *Angew. Chem., Int. Ed.*, 2011, **50**, 6606; (*b*) F.-S. Guo, J.-D. Leng, J.-L. Liu, Z.-S. Meng and M.-L. Tong, *Inorg. Chem.*, 2012, **51**, 405; (*c*) G. Lorusso, M. A. Palacios, G. S. Nichol, E. K. Brechin, O. Roubeau and M. Evangelisti, *Chem. Commun.*, 2012, **48**, 7592; (*d*) G. Lorusso, J. W. Sharples, E. Palacios, O. Roubeau, E. K. Brechin, R. Sessoli, A. Rossin, F. Tuna, E. J. L. McInnes, D. Collison and M. Evangelisti, *Adv. Mater.*, 2013, **25**, 4653; (*e*) K. Qian, B. Wang, Z. Wang, G. Su and S. Gao, *Acta Chim. Sin.*, 2013, **71**, 1022.

11 (*a*) Y. I. Spichkin, A. K. Zvezdin, S. P. Gubin, A. S. Mischenko and A. M. Tishin, *J. Phys. D: Appl. Phys.*, 2001, **34**, 1162; (*b*) M. Evangelisti and E. K. Brechin, *Dalton Trans.*, 2010, **39**, 4672; (*c*) R. Sessoli, *Angew. Chem., Int. Ed.*, 2012, **51**, 43; (*d*) J. W. Sharples and D. Collison, *Polyhedron*, 2013, **54**, 91; (*e*) Y.-Z. Zheng, G.-J. Zhou, Z. Zheng and R. E. P. Winpenny, *Chem. Soc. Rev.*, 2013, **43**, 1462.

12 (*a*) K. A. Gschneidner Jr and V. K. Pecharsky, *Annu. Rev. Mater. Sci.*, 2000, **30**, 387; (*b*) K. A. Gschneidner Jr, V. K. Pecharsky and A. O. Tsokol, *Rep. Prog. Phys.*, 2005, **68**, 1479.

13 (*a*) G. M. Sheldrick, *Acta Crystallogr.*, 2008, **A64**, 112; (*b*) A. L. Spek, *Acta Crystallogr.*, 2009, **D65**, 148.

14 (*a*) S. J. Clark, M. D. Segall, C. J. Pickard, P. J. Hasnip, M. J. Probert, K. Refson and M. C. Payne, *Z. Kristallogr.*, 2005, **220**, 567; (*b*) J. P. Perdew, K. Burke and M. Ernzerhof, *Phys. Rev. Lett.*, 1996, **77**, 3865; (*c*) J. D. Pack and M. J. Monkhorst, *Phys. Rev. B: Solid State*, 1977, **16**, 1748; (*d*) D. Zhang, R. K. Kremer, P. Lemmens, K. Y. Choi, J. Liu, M. H. Whangbo, H. Berger, Y. Skourski and M. Johnsson, *Inorg. Chem.*, 2011, **50**, 12877.

15 (*a*) T. Tahara, I. Nakai, R. Miyawaki and S. Matsubara, *Z. Kristallogr.*, 2007, **222**, 326; (*b*) H.-S. Sheu, W.-J. Shih, W.-T. Chuang, I.-F. Li and F.-S. Yeh, *J. Chin. Chem. Soc.*, 2010, **57**, 938; (*c*) K. Michiba, T. Tahara, I. Nakai, R. Miyawaki and S. Matsubara, *Z. Kristallogr.*, 2011, **226**, 518.

16 (*a*) M. Affronte, J. C. Lasjaunias and A. Cornia, *Eur. Phys. J. B*, 2000, **15**, 633; (*b*) M. Evangelisti, F. Luis, L. J. de Jongh and M. Affronte, *J. Mater. Chem.*, 2006, **16**, 2534.

17 (*a*) H. J. Koo and M. H. Whangbo, *Inorg. Chem.*, 2008, **47**, 4779; (*b*) S. T. Hatscher and W. Urland, *Angew.Chem., Int. Ed.*, 2003, **42**, 2862; (*c*) L. E. Roy and T. Hughbanks, *J. Am. Chem. Soc.*, 2006, **128**, 568; (*d*) J. Richter, J. Schulenberg and A. Honecher, *Quantum Magnetism in Two Dimensions: From Semi-classical Néel Order to Magnetic Disorder in Quantum Magnetism*, ed. U. Schollwöck, J. Richter, D. J. J. Farnell and R. F. Bishop, Springer, Berlin, 2004.